

**ASSESSING THE IMPACT OF CLIMATE CHANGE ON
CROP PRODUCTION IN THE INDIAN STATES OF
HIMACHAL PRADESH AND UTTAR PRADESH**

JYOTI SINGH



**CENTRE FOR ATMOSPHERIC SCIENCES
INDIAN INSTITUTE OF TECHNOLOGY DELHI**

NOVEMBER 2021

© Indian Institute of Technology Delhi (IITD), New Delhi, 2021

**ASSESSING THE IMPACT OF CLIMATE CHANGE ON
CROP PRODUCTION IN THE INDIAN STATES OF
HIMACHAL PRADESH AND UTTAR PRADESH**

by

JYOTI SINGH

Centre for Atmospheric Sciences

Submitted

**in fulfilment of the requirements of the degree of Doctor of Philosophy
to the**



INDIAN INSTITUTE OF TECHNOLOGY DELHI

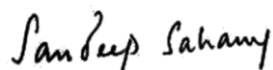
NOVEMBER 2021

Dedicated to my mother & Father
For their support, patience, and faith

Certificate

This is to certify that the thesis titled “*Assessing the impact of climate change on crop production in the Indian states of Himachal Pradesh and Uttar Pradesh*” being submitted by **Ms. Jyoti Singh** to the **Indian Institute of Technology Delhi** for the award of the degree of **Doctor of Philosophy**, is a record of original bonafide research work carried out by her. She has worked under our guidance and supervision and has fulfilled the requirements for the submission of this thesis.

The results presented in this thesis have not been submitted in part or full to any other University or Institute for the award of any degree or diploma.



PROF. SANDEEP SAHANY

Centre for Atmospheric Sciences

Indian Institute of Technology Delhi*



PROF. SAROJ KANTA MISHRA

Centre for Atmospheric Sciences

Indian Institute of Technology Delhi

**Currently at the Centre for Climate Research Singapore*

Acknowledgements

I want to express my sincere and profound gratitude to my supervisors, Prof. Sandeep Sahany and Prof. Saroj Kanta Mishra, for their invaluable guidance and wholehearted support. I am genuinely indebted to Prof. Sandeep Sahany, without whom this thesis would never have been possible. His approach towards a research question, emphasizing the subtext of the problem and tiny details in the search for a simple and elegant process, has taught me a great deal. I am thankful to him for being so generous with his time and immense patience with me. My collaboration and interactions with Prof. Alan Robock have improved my research immensely. I wish to thank him for his invaluable, accurate and elaborative feedbacks. I want to thank Prof. C.T. Dhanya for providing algorithms and valuable feedback on their incorporation into my research.

I am highly thankful to SRC members- Prof. Maithili Sharan, Prof. Vimlesh Pant, Prof. B.K. Panigrahi and Head CAS Prof. Krishna Achuta Rao for their helpful suggestions and advice. I want to extend my gratitude to all other faculty and administrative staff (especially Narendra Ji for his outstanding support) of CAS.

I want to gratefully acknowledge the Indian Institute of Technology Delhi (IITD) for providing me PhD fellowship and logistics during my PhD. I am grateful to the IITD Super Computing Facility for providing the computing resources for my PhD. I thank IITD, American Geophysical Union, and Asia Oceania Geosciences Society for providing the travel support to attend conferences and workshops during my PhD.

I am very fortunate to have some great people to share and discuss interesting ideas with me. Thanks to Tanvi Gupta for those long coffee and phone discussions. I am also thankful to Yajnaseni Dash, Papat Salunke, Raju Pathak, Ankur Dixit, Vivek Kumar, Abhishek Anand, Shoobhangi Tyagi, Shweta Chaube, Soumi Dutta, Rohit Kumar Choudhary and, Sudipta Ghosh for their support and discussions. Many have nothing directly to do with this thesis but have made my life very lively and meaningful. I want to thank my dearest friend Sweta for her unconditional support and love. I want to thank Panini and Devnil for their presence in my life for exciting and fun discussions.

I want to extend my wholehearted love and gratitude towards our campus dogs (PubG, Peepani, Bachchan, Devil, Laila, Vindy, Lalu, and the Gupta-store gang). They have made my stay at IIT Delhi much happier and joyous. I want to thank my precious [cat] "Dukie" for being on my side in the long and alone times of the pandemic in IIT Delhi.

A special thanks to my dearest friend and partner, Abhishek Das. He has always enthralled curiosity in me about science through his unworldly attitude and most straightforward possible explanations of a

scientific phenomenon. I want to mention and remember my life coaches, late Aji and late Bade papa, for always encouraging and boosting my sense of freedom and curiosity.

Finally, I wish to express my deep appreciation to my mother, father, brother, sister and big joint family for their patience, unconditional love, and support during this thesis. This thesis is dedicated to all of them and science.

Jyoti Singh

Abstract

Food production in India (having one-sixth of the world population) is already affected by changing climate and is expected to accelerate in the future due to an increase in temperature, change in rainfall pattern, and increased frequency and intensity of extreme events. India is highly vulnerable to the impacts of climate change because of high population density, large agricultural workforce and limited adaptive capacity. Furthermore, increasing population (from current levels of ~1.3 to ~1.65 billion by 2060) and consumption growth coupled with climate change will increase food security risk. With these underlying uncertainties and challenges, it becomes imperative to assess the impact of global warming-related climate change on food production. However, most of the studies assessing the climate change impacts on agriculture are site-specific, use few coarse-resolution GCM data, and ignore farm management variability. Studies utilising GCM data lack in capturing the uncertainty in future projections because considered GCMs are significantly less in number. None of the studies in India have explored the potential strategies (e.g., geoengineering) to combat climate change in fragile ecosystems (e.g., Himalayas).

The research in this thesis focuses on understanding the impact of climate change on major crops of the two most vulnerable regions, the Himalayas (fragile ecosystem, rapid warming, and marginal adaptive capacity) and Indo-Gangetic plains (high population, already stressed natural resources and marginal adaptive capacity) of India. To begin with, we first evaluated four statistical downscaling techniques (QM, KNN_p, KNN and SVM-KNN) to be used in agriculture impact assessment. Coarse-resolution GCM data are not suitable to be directly used for agriculture-related impact assessment studies, especially for developing regions having diverse crop management practices. QM and KNN_p use rainfall to downscale rainfall. In contrast, KNN and SVM-KNN use large scale atmospheric variables (e.g., air temperature, specific humidity, wind speed, geopotential height at various pressure levels) to downscale rainfall. We evaluated the performance of the downscaling methods, their ability to capture annual rainfall amount, spatial pattern, seasonal and daily variability, extreme rainfall amount and some agriculture-specific metrics. We found that, overall, all the techniques perform (using correlation coefficient, root mean square error and mean absolute error) satisfactorily. SVM-KNN and KNN fail to capture the seasonal and daily variability and extremes of the monsoon (JJAS) rainfall, whereas QM outperforms all the other techniques for the same. Wet day fraction, wet spell length, average wet spell rainfall and dry spell length were used to evaluate the usefulness of these techniques in agriculture applications. QM performs best for the agriculture-specific metrics, and SVM-KNN and KNN significantly overestimate. Based on our analysis, we chose QM to downscale the GCM outputs and use it for further analysis in the subsequent chapters.

Next, the impact of global warming on land suitability of deciduous fruit over Himachal Pradesh was assessed using Hadley Global Environment Model 2 - Earth System (HadGEM2-ES) and

Max Planck Institute Earth System Model (MPI-ESM) under RCP4.5 from CMIP5. A corresponding stratospheric geoengineering scenario (G3 from GeoMIP5), proposed to combat the harmful effects of global warming, was also assessed for the same models. We used the period 2055–2069 (with the highest geoengineering forcing [switched-on]) and the period 2075–2089 (beginning five years into the termination phase [switched-off]) for analysis. We found that stratospheric geoengineering would suppress the increase in temperature under RCP4.5 scenario to some extent during both switched-on and switched-off periods. However, if the geoengineering were terminated, the rate of temperature increase would be higher than RCP4.5. The agroclimatically suitable area is projected to shift north-eastwards (to higher elevations) under RCP4.5 as well as G3 during both periods. However, geoengineering would restrict the shift during the switched-on period, and areas of Shimla and Mandi districts (most suitable under the current climate) would not be lost due to global warming. Even during the switched-off period, before the climate returned to RCP4.5 levels, the above areas would, although to a lesser extent, have reduced harmful climate effects from global warming. However, the area of suitable land (the intersection of suitable soil and agroclimatic suitability) would decrease in both periods for RCP4.5 and G3, because the high-elevation regions that become agroclimatically suitable are mostly rocky (unfit for cultivation). Geoengineering could benefit deciduous fruit production by reducing the intensity of global warming. However, if geoengineering were terminated abruptly, the rate of temperature change would be quite high, leading to a rapid change in land suitability and might result in total crop failure in a shorter period than RCP4.5.

In the next part of the thesis, the impact of climate change on Kharif season rice using more than a thousand crop-climate scenarios in Uttar Pradesh was carried out. Uttar Pradesh is divided into nine agroecological zones (AEZs) based on climate and soil. The study area of Uttar Pradesh has a total of 342 grids of 25 km x 25 km grid-spacing, and each AEZ contains a given number of grids. A total of 1152 (16 x 4 x 2 x 3 x 3) experiments were designed using a combination of planting dates (3), rice cultivars (4), GCMs (16), irrigation conditions (2), and CO₂ concentration (3; historical, Shared Socio-economic Pathway 245 [SSP245] and SSP585) for a total of 342 grids. A gridded framework was designed to run the site-specific CERES-Rice model in a gridded environment. The simulations were carried out by forcing CERES-Rice with bias-adjusted and downscaled CMIP6 GCMs for historical, SSP245 and SSP585. In addition, the CO₂ fertilization effect is quantified by performing sensitivity experiments that include forcing CERES-Rice with a constant CO₂ value representative of 2005 (average of 1995-2014) and climates from SSP245 and SSP585 for all the three future periods for one planting scenario. The CERES-Rice simulations were performed for the historical (1995-2014) and three future periods (2030s [2026-2035], 2050s [2046-2055], and 2090s [2090-2099]) for the two SSPs. Phenology (anthesis and maturity), irrigation amount, crop evapotranspiration (ET), crop transpiration (EP), soil evaporation (ES), yield and water use efficiency (WUE) were evaluated and assessed for all AEZs.

Next, we evaluated CERES-Rice outputs for historical runs (1995-2014), forced with bias-adjusted and downscaled GCM climate with IMD-forced simulations. The output variables were averaged for early, mid, and late planting (25 June, 5 July, and 15 July), four cultivars, and aggregated for each AEZ for irrigated and rainfed rice. We found that the CERES-Rice simulations are dependent on input climate variables. Bias-adjusted and downscaled data produce match well with IMD data, yet residual biases in the frequency, intensity, and distribution of rainfall affect the related crop model outputs. Irrigation requirement and soil moisture (that affects ES, EP, ET, irrigation, yield and WUE) heavily depend on rainfall, hence their performance is affected. The uncertainties are higher in rainfed rice because it solely depends upon rainfall for crop water requirement, unlike irrigated rice, which is not limited by water availability. The model performance was found to vary with planting dates and AEZs.

Next, the impact of climate change under SSP245 and SSP585 was assessed for irrigated and rainfed rice for all the planting seasons. Results based on the multi-model mean (MMM) of 16 GCMs project increased rainfed rice yield in AEZs of western Uttar Pradesh due to increased rainfall, however, in eastern Uttar Pradesh, yield decreases under both SSPs. Irrigated rice yield decreases in all AEZs under both SSPs due to increase in temperature and decrease in the length of growing period, and by 2090s the reduction is up to 20%. For irrigated rice, lowest decrease in yield is in early planting, and for rainfed rice, highest increase in yield is in early planting. Irrigation decreases monotonically from early to the end of the century due to increased rainfall and a decrease in crop ET. The reduction in crop ET is associated with reduced vapour deficit (due to increased rain) and elevated CO₂ (reduced stomata opening). Water use efficiency (WUE) increases for both irrigated and rainfed rice from 2030s to 2050s and decreases by 2090s. The elevated CO₂ concentration increases rice yield for both rainfed and irrigated conditions. However, the combination of increased rainfall and CO₂ levels seems to be more beneficial for rainfed rice than irrigated rice. The CO₂ fertilization effect in rainfed rice is not spatially uniform as that in irrigated rice. The highest increase in rainfed rice yield due to elevated CO₂ is projected over semi-arid and dry sub-humid AEZs of Uttar Pradesh. Overall, our analysis finds that rainfed rice yield is projected to increase in western Uttar Pradesh, whereas decrease in eastern Uttar Pradesh under climate change. Irrigated rice yield is projected to decrease in all the AEZs of the state under climate change.

सार

भारत (दुनिया की आबादी का छठा हिस्सा) में खाद्य उत्पादन पहले से ही बदलती जलवायु से प्रभावित है और भविष्य में तापमान में वृद्धि, वर्षा पैटर्न में बदलाव और अतिविषम जलवायु घटनाओं की आवृत्ति और तीव्रता में वृद्धि के कारण इसमें और तेजी आने की सम्भावना है। उच्च जनसंख्या घनत्व, कृषि पर निर्भरता और सीमित अनुकूली क्षमता के कारण भारत जलवायु परिवर्तन के प्रभावों के प्रति अत्यधिक संवेदनशील है। इसके अलावा, बढ़ती जनसंख्या (2060 तक ~1.3 से बढ़कर ~1.65 बिलियन) और जलवायु परिवर्तन के साथ खपत वृद्धि से खाद्य सुरक्षा जोखिम और बढ़ जाएगा। इन अंतर्निहित अनिश्चितताओं और चुनौतियों के साथ, खाद्य उत्पादन पर ग्लोबल वार्मिंग से संबंधित जलवायु परिवर्तन के प्रभाव का आकलन करना अनिवार्य हो जाता है। हालांकि, कृषि पर जलवायु परिवर्तन के प्रभावों का आकलन करने वाले अधिकांश अध्ययन साइट-विशिष्ट हैं, कुछ कम रिज़ॉल्यूशन वाले GCM डेटा का उपयोग करते हैं, और कृषि प्रबंधन परिवर्तनशीलता को अनदेखा करते हैं। GCM डेटा का उपयोग करने वाले अध्ययनों में भविष्य के अनुमानों में अनिश्चितता को पकड़ने में कमी होती है क्योंकि प्रयोग किये गए GCM संख्या में काफी कम होते हैं। अभी तक किसी भी अध्ययन में भारत के अतिसंवेदनशील पारिस्थितिक तंत्र (जैसे, हिमालय) में जलवायु परिवर्तन से निपटने के लिए संभावित रणनीतियों (जैसे, जियोइंजीनियरिंग) का पता नहीं लगाया है।

यह थीसिस भारत के दो अति संवेदनशील क्षेत्रों, हिमालय (संवेदनशील पारिस्थितिकी तंत्र, तेजी से गर्म होने और सीमांत अनुकूली क्षमता) और भारत-गंगा के मैदानों (उच्च जनसंख्या, प्राकृतिक संसाधनों पर पूर्व से ही दबाव) की प्रमुख फसलों पर जलवायु परिवर्तन के प्रभाव को समझने पर केंद्रित है। सबसे पहले, हमने कृषि प्रभाव मूल्यांकन में उपयोग की जाने वाली चार स्टैटिस्टिकल डाउनस्केलिंग तकनीकों (QM, KNN_p, KNN और SVM-KNN) का मूल्यांकन किया। कम रिज़ॉल्यूशन वाले GCM डेटा कृषि से संबंधित प्रभाव मूल्यांकन अध्ययनों के लिए सीधे उपयोग करने के लिए उपयुक्त नहीं हैं, विशेष रूप से विविध फसल प्रबंधन प्रथाओं वाले विकासशील क्षेत्रों के लिए। QM और KNN_p वर्षा का उपयोग करके वर्षा को डाउनस्केल करते हैं। इसके विपरीत, KNN और SVM-KNN बड़े पैमाने के वायुमंडलीय वेरिएबल्स (जैसे, हवा का तापमान, विशिष्ट आर्द्रता, हवा की गति, विभिन्न दबाव स्तरों पर भू-संभावित ऊंचाई) का उपयोग करके वर्षा को डाउनस्केल करते हैं। हमने डाउनस्केलिंग विधियों के प्रदर्शन, वार्षिक वर्षा राशि, स्थानिक पैटर्न, मौसमी और दैनिक परिवर्तनशीलता, अतिविषम वर्षा राशि और कुछ कृषि-विशिष्ट मेट्रिक्स को पकड़ने की उनकी क्षमता का मूल्यांकन किया। हमने पाया कि, कुल मिलाकर, सभी तकनीकें संतोषजनक ढंग से प्रदर्शन करती हैं (correlation coefficient, root mean square error and mean absolute error का उपयोग करके)। SVM-KNN और KNN मौसमी और दैनिक परिवर्तनशीलता और मानसून (JJAS) वर्षा की चरम सीमा को पकड़ने में विफल रहते हैं, जबकि QM उसी के लिए अन्य सभी तकनीकों से बेहतर प्रदर्शन करता है। कृषि अनुप्रयोगों में इन तकनीकों की उपयोगिता का मूल्यांकन करने के लिए वेट डे फ्रैक्शन, वेट स्पेल लेंथ, मीन वेट स्पेल रेनफॉल और ड्राई स्पेल की अवधि का उपयोग किया गया था। QM कृषि-विशिष्ट मेट्रिक्स के लिए सबसे अच्छा प्रदर्शन करता है, और KNN और SVM-KNN काफी अधिक अनुमान लगाते हैं। हमारे विश्लेषण के आधार पर, हमने GCM आउटपुट को डाउनस्केल करने के लिए QM को चुना और बाद के अध्यायों में आगे के विश्लेषण के लिए इसका इस्तेमाल किया।

इसके बाद, हिमाचल प्रदेश पर पर्णपाती फलों की भूमि की उपयुक्तता पर ग्लोबल वार्मिंग के प्रभाव का आकलन हैडली ग्लोबल एनवायरनमेंट मॉडल 2 - अर्थ सिस्टम (HadGEM2-ES) और मैक्स प्लैंक इंस्टीट्यूट अर्थ सिस्टम मॉडल (MPI-ESM) के तहत RCP4.5 (समिपु) से किया गया। ग्लोबल वार्मिंग के हानिकारक प्रभावों से

निपटने के लिए प्रस्तावित स्ट्रैटोस्फेरिक जियोइंजीनियरिंग (GeoMIP5 से G3) का भी उन्हीं मॉडलों के लिए मूल्यांकन किया गया था। हमने विश्लेषण के लिए 2055-2069 (उच्चतम जियोइंजीनियरिंग फोर्सिंग [स्विच-ऑन] के साथ) और 2075-2089 की अवधि (टर्मिनेशन चरण [स्विच-ऑफ] में शुरुआत के पांच साल) का उपयोग किया। हमने पाया कि स्ट्रैटोस्फेरिक जियोइंजीनियरिंग स्विच-ऑन और स्विच-ऑफ दोनों अवधियों के दौरान कुछ हद तक RCP4.5 परिदृश्य के तहत तापमान में वृद्धि को दबा देगी। हालाँकि, यदि जियोइंजीनियरिंग को समाप्त कर दिया गया, तो तापमान वृद्धि की दर RCP4.5 से अधिक होगी। कृषि जलवायु की दृष्टि से उपयुक्त क्षेत्रों का दोनों अवधियों के दौरान RCP4.5 के साथ-साथ G3 के तहत उत्तर-पूर्व की ओर (उच्च ऊंचाई पर) स्थानांतरित होने का अनुमान है। हालाँकि, जियोइंजीनियरिंग स्विच-ऑन अवधि के दौरान शिफ्ट को प्रतिबंधित कर देगी, और शिमला और मंडी जिलों के क्षेत्र (वर्तमान जलवायु के तहत सबसे उपयुक्त) ग्लोबल वार्मिंग के कारण नष्ट नहीं होंगे। स्विच-ऑफ अवधि के दौरान भी, जलवायु के RCP4.5 के स्तर पर लौटने से पहले, उपरोक्त क्षेत्रों ने, हालाँकि कुछ हद तक, ग्लोबल वार्मिंग से हानिकारक जलवायु प्रभावों को कम किया होगा। हालाँकि, उपयुक्त भूमि का क्षेत्र (उपयुक्त मिट्टी और कृषि जलवायु उपयुक्तता का प्रतिच्छेदन) RCP4.5 और G3 दोनों अवधियों में घट जाएगा, क्योंकि उच्च ऊंचाई वाले क्षेत्र जो कृषि के लिए उपयुक्त हो जाते हैं, वे ज्यादातर चट्टानी (खेती के लिए अनुपयुक्त) होते हैं। ग्लोबल वार्मिंग की तीव्रता को कम करके जियोइंजीनियरिंग पर्णपाती फलों के उत्पादन को लाभ पहुंचा सकती है। हालाँकि, अगर जियोइंजीनियरिंग को अचानक समाप्त कर दिया गया, तो तापमान परिवर्तन की दर काफी अधिक होगी, जिससे भूमि की उपयुक्तता में तेजी से बदलाव आएगा और इसके परिणामस्वरूप RCP4.5 की तुलना में कम अवधि में कुल फसल खराब हो सकती है।

थीसिस के अगले भाग में, उत्तर प्रदेश में एक हजार से अधिक फसल-जलवायु परिदृश्यों का उपयोग करके खरीफ मौसम के चावल पर जलवायु परिवर्तन के प्रभाव का अध्ययन किया गया। उत्तर प्रदेश को जलवायु और मिट्टी के आधार पर नौ एग्रो-इकोलॉजिकल ज़ोन्स (AEZ) में विभाजित किया गया है। उत्तर प्रदेश के अध्ययन क्षेत्र में 25 किमी x 25 किमी ग्रिड-स्पेसिंग के कुल 342 ग्रिड हैं, और प्रत्येक एईजेड में कुछ ग्रिड हैं। कुल 1152 (16 x 4 x 2 x 3 x 3) प्रयोग, प्रत्यारोपण तिथियों (3), चावल की किस्मों (4), GCM(16), सिंचाई की स्थिति (2), और CO₂ कंसंट्रेशन (3 ; हिस्टोरिकल, शेयर्ड सोसिओ-इकनोमिक पाथवे 245[SSP245] और SSP585), कुल ३४२ ग्रिड के लिए किए गए हैं। ग्रिड वाले वातावरण में साइट-विशिष्ट CERES-Rice मॉडल को चलाने के लिए एक ग्रिड फ्रेमवर्क तैयार किया गया है। हिस्टोरिकल, SSP245 और SSP585 के लिए बायस-अडजस्टेड और डाउनस्केल्ड CMIP6 GCM के साथ CERES-Rice में इनपुट करके सिमुलेशन किए गए हैं। इसके अलावा, CO₂ फर्टिलाइजेशन इफेक्ट को संवेदनशीलता प्रयोगों द्वारा निर्धारित किया गया है जिसमें 2005 (1995-2014 का औसत) के CO₂ कंसंट्रेशन को एक रोपण परिदृश्य के लिए, भविष्य जलवायु (SSP245 और SSP585) में सभी तीन की अवधि के लिए के साथ CERES-Rice सिमुलेट करना शामिल है। CERES-Rice सिमुलेशन हिस्टोरिकल (1995-2014) और दो SSP के तीन भविष्य की अवधि (2030 [2026-2035], 2050 [2046-2055], और 2090 [2090-2099]) के लिए किए गए हैं। सभी AEZ के लिए फेनोलॉजी (एंथिसिस और मेट्यूरीटी), सिंचाई राशि, फसल वाष्पीकरण (ET), फसल वाष्पोत्सर्जन (EP), मिट्टी वाष्पीकरण (ES), उपज और जल उपयोग दक्षता (WUE) का आकलन किया गया है।

इसके बाद, हमने हिस्टोरिकल रन (1995-2014) के लिए, IMD इनपुट वाले सिमुलेशन के साथ पूर्वाग्रह-समायोजित और डाउनस्केल्ड GCM जलवायु इनपुट वाले सिमुलेशन वाले CERES-Rice के आउटपुट का आकलन किया। सिंचित और वर्षा-आधारित आउटपुट वेरिफेबल्स को शुरुआती, मध्य और देर से प्रत्यारोपण (25 जून, 5 जुलाई और 15 जुलाई), और चार किस्मों का हर AEZ के लिए औसत निकला। हमने पाया कि CERES-Rice सिमुलेशन इनपुट जलवायु वेरिफेबल्स पर निर्भर हैं। बायस-अडजस्टेड और डाउनस्केल्ड डेटा उत्पादन IMD डेटा के

साथ अच्छी तरह से मेल खाते हैं, फिर भी वर्षा की आवृत्ति, तीव्रता और वितरण में अवशिष्ट पूर्वाग्रह संबंधित फसल मॉडल आउटपुट को प्रभावित करते हैं। सिंचाई की आवश्यकता और मिट्टी की नमी (जो ES, EP, ET, सिंचाई, उपज और WUE को प्रभावित करती है) बहुत अधिक वर्षा पर निर्भर करती है, इसलिए उनका प्रदर्शन प्रभावित होता है। वर्षा-आधारित चावल में अनिश्चितताएं अधिक होती हैं क्योंकि यह सिंचित चावल जो पानी की उपलब्धता से सीमित नहीं है के विपरीत पूरी तरह से फसल की पानी की आवश्यकता के लिए वर्षा पर निर्भर करता है। प्रत्यारोपण की तारीखों और AEZ के साथ मॉडल का प्रदर्शन अलग-अलग पाया गया।

इसके बाद, सभी प्रत्यारोपण मौसमों के लिए सिंचित और वर्षा-आधारित चावल के लिए SSP245 और SSP585 के तहत जलवायु परिवर्तन के प्रभाव का आकलन किया गया। 16 GCM के बहु-मॉडल माध्य (MMM) के आधार पर परिणाम पश्चिमी उत्तर प्रदेश के AEZ में वर्षा आधारित चावल की पैदावार में वृद्धि का प्रक्षेपण करते हैं, हालांकि, पूर्वी उत्तर प्रदेश में, दोनों SSP के तहत उपज घटने का प्रक्षेपण करते हैं। तापमान में वृद्धि और फसल अवधि की लंबाई में कमी के कारण दोनों SSP के तहत सभी AEZ में सिंचित चावल की उपज घट जाती है और 2090 तक कमी 20% तक होने का प्रक्षेपण है। सिंचित चावल के लिए, उपज में सबसे कम कमी जल्दी रोपण में होती है, और वर्षा-आधारित चावल के लिए, उपज में सबसे अधिक वृद्धि जल्दी रोपण में होती है। वर्षा में वृद्धि और फसल के ET में कमी के कारण सदी के अंत तक सिंचाई एकरस रूप से कम हो जाती है। फसल के ET में कमी, वाटर डेफिसिट में कमी (बारिश बढ़ने के कारण) और बढ़े हुए CO₂ (रंधों के खुलने में कमी) से जुड़ी है। 2030 से 2050 तक सिंचित और वर्षा-आधारित चावल दोनों के लिए जल उपयोग दक्षता (WUE) बढ़ जाने और 2090 तक घट जाने का प्रक्षेपण है। CO₂ की उच्च सांद्रता वर्षा-आधारित और सिंचित दोनों स्थितियों में चावल की उपज को बढ़ाती है। हालांकि, बढ़ी हुई वर्षा और CO₂ के स्तर का संयोजन सिंचित चावल की तुलना में वर्षा-आधारित चावल के लिए अधिक फायदेमंद प्रतीत होता है। वर्षा-आधारित चावल में CO₂ निषेचन प्रभाव सिंचित चावल की तरह स्थानिक रूप से एक समान नहीं है। उत्तर प्रदेश के अर्ध-शुष्क और शुष्क उप-आर्द्र AEZ में बढ़े हुए CO₂ के कारण वर्षा-आधारित चावल की उपज में सबसे अधिक वृद्धि का अनुमान है। कुल मिलाकर, हमारे विश्लेषण से पता चलता है कि पश्चिमी उत्तर प्रदेश में वर्षा आधारित चावल की पैदावार बढ़ने का अनुमान है, जबकि पूर्वी उत्तर प्रदेश में जलवायु परिवर्तन के तहत कमी आई है। जलवायु परिवर्तन के तहत राज्य के सभी AEZ में सिंचित चावल की पैदावार घटने का अनुमान है।

Table of Contents

Certificate	i
Acknowledgements	ii
Abstract (English)	iv
Abstract (Hindi)	vii
Table of Contents	x
List of Figures	xiii
List of Tables	xx
List of Acronyms	xxi
1. Introduction.....	1
1.1 Climate change.....	1
1.2 Climate and crop processes.....	4
1.3 Simulating crop growth using crop models	5
1.4 Impact of climate change on Indian agriculture.....	6
1.4.1 Rice crops.....	7
1.4.2 Deciduous fruits	8
1.5 Research Problem & Objectives	8
2. Evaluation and selection of statistical downscaling techniques	11
2.1 Introduction.....	11
2.2 Study area and data	12
2.2.1 Study area.....	12
2.2.2 Observation data	12
2.2.3 NCEP/NCAR reanalysis	13
2.3 Methodology	13
2.3.1 Bias adjustment.....	13
2.3.2 Principal component analysis (PCA)	14
2.3.3 Quantile mapping based statistical downscaling (QM).....	15
2.3.4 K-nearest neighbour (KNN and KNN _p).....	16
2.3.5 Coupled SVM and KNN (SVM-KNN).....	17
2.4 Results and Discussion	17

2.4.1 Performance analysis of downscaling methods	18
2.4.2 Rainfall biases, variability in monthly and daily rainfall	19
2.4.3 Extreme rainfall.....	23
2.4.4 Indices relevant to agricultural applications	24
2.5 Summary	28
3. Assessment of the impact of global warming and geoengineering on deciduous fruit land suitability	30
3.1 Introduction.....	30
3.2 Data.....	33
3.3 Methodology	35
3.3.1 Bias adjustment and statistical downscaling	35
3.3.2 Hourly temperature conversion.....	36
3.3.3 Calculating chill and heat requirements.....	37
3.4 Results and Discussion	39
3.4.1 Changes in surface temperature under RCP4.5 and G3	39
3.4.2 Changes in chill and heat requirement under RCP4.5 and G3.....	42
3.4.3 Changes in agroclimatic and land suitability under RCP4.5 and G3	46
3.5 Summary	50
4. Evaluating CERES-Rice simulations for rainfed and irrigated rice.....	53
4.1 Introduction.....	53
4.2 Data and Model.....	55
4.2.1 Study area.....	55
4.2.2 Observed climate data.....	56
4.2.3 CMIP6 data	57
4.2.4 CERES-Rice model.....	58
4.2.5 Crop management data.....	59
4.3 Methodology	62
4.3.1 CMIP6 model performance and selection.....	62
4.3.2 Bias adjustment and statistical downscaling	64

4.3.3 CERES-Rice model simulation.....	64
4.4 Results and Discussion	65
4.4.1 Seasonal temperature and phenology.....	66
4.4.2 Seasonal rainfall, irrigation, and crop water requirement	68
4.4.3 Yield.....	72
4.4.4 Water use efficiency (WUE).....	73
4.5 Summary	74
5. Assessing the impact of global warming on rainfed and irrigated rice.....	77
5.1 Introduction.....	77
5.2 Methodology	79
5.3 Results and Discussion	80
5.3.1 Change in temperature and phenology.....	80
5.3.2 Change in rainfall.....	86
5.3.3 Change in crop water requirements	86
5.3.4 Changes in yield.....	93
5.3.5 Changes in water use efficiency.....	98
5.3.6 CO ₂ fertilization	101
5.4 Summary	103
6. Conclusions and future work.....	106
6.1 Conclusions.....	106
6.2 Future work.....	110
References.....	111
Appendix.....	130
Curriculum - Vitae.....	142

List of Figures

FIGURE 2-1 CDF FOR DAILY JJAS RAINFALL OF IMD, NCEP AND BIAS ADJUSTED NCEP FOR THE PERIOD OF 1979-1999	14
FIGURE 2-2 PRINCIPAL COMPONENTS OF THE NCEP PREDICTOR SET (FOR KNN AND SVM-KVV) THAT EXPLAINS 95% VARIANCE FOR THE CALIBRATION PERIOD (1979-1999).	15
FIGURE 2-3 FLOWCHART OF THE FOUR DOWNSCALING TECHNIQUES, NAMELY, QM, KNN AND SVM-KNN	17
FIGURE 2-4 PERFORMANCE ANALYSIS OF DOWNSCALING METHODS USING (I) CORRELATION COEFFICIENT, (II) ROOT MEAN SQUARE ERROR, AND (III) MEAN ABSOLUTE ERROR.....	19
FIGURE 2-5 MEAN ANNUAL RAINFALL FOR A) OBSERVATION, AND BIASES IN B) QM, C) KNN _p , D) KNN, AND E) SVM-KNN FOR THE VALIDATION PERIOD (2000-2009)	20
FIGURE 2-6 BOX PLOTS SHOWING VARIABILITY IN MONTHLY RAINFALL CONSIDERING INDIVIDUAL GRID-POINTS OVER THE STUDY REGION WITHOUT ANY SPATIAL AVERAGING FOR THE VALIDATION PERIOD (2000-2009) FOR OBSERVATION AND ALL THE DOWNSCALING TECHNIQUES. LOWER AND UPPER EDGES OF THE BOX ARE 25TH AND 75TH PERCENTILE, RESPECTIVELY. THE DOTTED CIRCLE CONTAINED WITHIN THE BOX REPRESENTS THE MEDIAN OF THE MONTHLY RAINFALL. THE LOWER AND UPPER WHISKERS ARE THE LOWEST AND HIGHEST EXTREMES NOT CONSIDERED OUTLIERS, OUTLIERS ARE NOT SHOWN IN THIS PLOT. RED-LINE DENOTES IMD MEDIAN VALUE FOR EACH MONTH OVER THE STUDY REGION.	21
FIGURE 2-7 BOX PLOTS SHOWING VARIABILITY IN DAILY JJAS RAINFALL CONSIDERING ALL GRID-POINTS OVER THE STUDY REGION WITHOUT ANY SPATIAL AVERAGING FOR THE VALIDATION PERIOD (2000-2009) FOR OBSERVATION AND ALL THE DOWNSCALING METHODS. LOWER AND UPPER EDGES OF THE BOX ARE 25TH AND 75TH PERCENTILE, RESPECTIVELY. THE DOTTED CIRCLE CONTAINED WITHIN THE BOX REPRESENTS THE MEDIAN OF THE DAILY RAINFALL. THE LOWER AND UPPER WHISKERS ARE THE LOWEST AND HIGHEST EXTREMES NOT CONSIDERED OUTLIERS; OUTLIERS ARE NOT SHOWN IN THIS PLOT. DASHED RED LINE REPRESENTS RAINFALL OF MAGNITUDE 2.5MM (WET DAY).	22
FIGURE 2-8 99TH PERCENTILE RAINFALL (MM) FROM (A) OBSERVATION, AND THE RESPECTIVE BIASES (MM) IN THE DOWNSCALED RAINFALL IN (B) QM, (C) KNN _p , (D) KNN, AND (E) SVM-KNN FOR THE VALIDATION PERIOD (2000-2009).....	23
FIGURE 2-9 DESCRIPTION OF AGRICULTURE SPECIFIC METRICS USED TO EVALUATE THE PERFORMANCE OF THE FOUR DOWNSCALING TECHNIQUES	24
FIGURE 2-10 WET DAY FRACTION FROM (A) OBSERVATION, AND BIASES IN DOWNSCALED RAINFALL IN (B) QM, (C) KNN _p , (D) KNN, AND (E) SVM-KNN FOR VALIDATION PERIOD (2000-2009)	25
FIGURE 2-11 WET SPELL LENGTH (DAYS) FROM (A) OBSERVATION, AND BIASES (DAYS) IN DOWNSCALED RAINFALL IN (B) QM, (C) KNN _p , (D) KNN, AND (E) SVM-KNN FOR VALIDATION PERIOD (2000-2009)	26
FIGURE 2-12 MEAN WET SPELL RAINFALL ACCUMULATION (MM) FROM (A) OBSERVATION, AND BIASES (MM) IN DOWNSCALED RAINFALL IN (B) QM, (C) KNN _p , (D) KNN, AND (E) SVM-KNN FOR VALIDATION PERIOD (2000-2009).....	27
FIGURE 2-13 DRY SPELL LENGTH (DAYS) FROM (A) OBSERVATION, AND BIASES (DAYS) IN DOWNSCALED RAINFALL IN (B) QM, (C) KNN _p , (D) KNN, AND (E) SVM-KNN FOR VALIDATION PERIOD (2000-2009)	28
FIGURE 3-1 LOCATION OF THE STUDY AREA (HIMACHAL PRADESH, INDIA). THE DOTTED LINES (VIOLET, BLACK AND RED) DIVIDES THE FOUR PHYSIOGRAPHIC REGIONS (GREATER HIMALAYAS, LESSER HIMALAYAS, OUTER HIMALAYAS AND PIEDMONT PLAINS). THE OVERLAID GRID BOXES REPRESENT THE RESOLUTION (25 KM) AT WHICH THE STUDY IS CARRIED OUT.	30

FIGURE 3-2 EXPERIMENT DESIGN OF THE SULPHATE GEOENGINEERING SCENARIO G3. BRANCHING OF THE RCP4.5 RUNS STARTING IN 2020, TO INJECT SULPHATE AEROSOLS IN THE STRATOSPHERE TO NEUTRALIZE THE INCREASE OF THE CORRESPONDING GLOBAL MEAN RADIATIVE FORCING DUE TO INCREASED CO ₂ LEVELS IN RCP4.5, THE SULPHATE AEROSOL INJECTION IS CEASED AFTER 2069. SOURCE: (KRAVITZ ET AL., 2011).....	33
FIGURE 3-3 DAILY MAXIMUM TEMPERATURE (A, B, C), DAILY MEAN TEMPERATURE (D, E, F), AND DAILY MINIMUM TEMPERATURE (G, H, I) FOR PRINCETON GLOBAL FORCING DATA, DOWNSCALED HADGEM2-ES AND DOWNSCALED MPI-ESM-LR, RESPECTIVELY.	35
FIGURE 3-4 ESTIMATED DIURNAL CYCLE FOR A) LOWER ELEVATIONS IN SOUTHERN HIMACHAL PRADESH (SIRMAUR DISTRICT), B) HIGHER ELEVATIONS IN NORTHERN HIMACHAL PRADESH (LAHUL & SPITI DISTRICT) FOR THE MONTHS OF JANUARY (BLUE), APRIL (BLACK), JULY (MAGENTA), AND OCTOBER (RED).....	37
FIGURE 3-5 THE CRITICAL PROCESS OF THE DYNAMIC MODEL IS PRESENTED FOR HOURLY TEMPERATURE, T (°C). INITIAL HOURLY TEMPERATURE (T STATE) PROMPTS THE CREATION OF AN INTERMEDIATE PRODUCT THAT CAN BE NULLIFIED BY SUBSEQUENT WARM TEMPERATURE. HOWEVER, THE INTERMEDIATE PRODUCT IS CONVERTED INTO AN IRREVERSIBLE CHILL PORTION WHEN THE ACCUMULATED THRESHOLD REACHES A CERTAIN THRESHOLD.	38
FIGURE 3-6 SIMULATED CHANGES IN DAILY MAXIMUM TEMPERATURE (A, B, C, D), DAILY MEAN TEMPERATURE (E, F, G, H), AND DAILY MINIMUM TEMPERATURE (I, J, K, L) UNDER RCP4.5 AND G3 FOR HADGEM2-ES AND MPI-ESM-LR FOR PERIOD1 (2055-2069; GEOENGINEERING SWITCHED ON).	40
FIGURE 3-7 SIMULATED CHANGES IN DAILY MAXIMUM TEMPERATURE (A, B, C, D), DAILY MEAN TEMPERATURE (E, F, G, H), AND DAILY MINIMUM TEMPERATURE (I, J, K, L) UNDER RCP4.5 AND G3 FOR HADGEM2-ES (FIRST 2 COLUMNS) AND MPI-ESM-LR (LAST 2 COLUMNS) FOR PERIOD2 (2075-2089; GEOENGINEERING SWITCHED OFF).	41
FIGURE 3-8 OROGRAPHY MAP OF HIMACHAL PRADESH DERIVED FROM SHUTTLE RADAR TOPOGRAPHY MISSION DIGITAL ELEVATION MODEL AT 1 KM RESOLUTION SHOWING ELEVATION IN METRES, OVERLAID WITH SUITABLE SOIL (RED DOTS) AND THE THREE DIVIDED REGIONS (I, II AND III).	42
FIGURE 3-9 AVERAGE WINTER CHILL ACCUMULATION (CP) (A, B, C), AND AVERAGE SPRING HEAT ACCUMULATION (D, E, F) FOR HADGEM2-ES, MPI-ESM-LR AND AVERAGE OF BOTH THE MODELS FOR THE HISTORICAL PERIOD (1910-2005).	43
FIGURE 3-10 IMPACT OF GLOBAL WARMING AND GEOENGINEERING ON CHILL ACCUMULATION (CP) IN PERIOD1 (A, B, C), AND PERIOD 2 (D, E, F) FOR THE AVERAGE OF HADGEM2-ES AND MPI-ESM-LR OVER HIMACHAL PRADESH, INDIA. THE UNHATCHED AREA SHOWS THAT THE DIFFERENCE OF CP FOR THE GIVEN SCENARIOS IS STATISTICALLY SIGNIFICANT AT 99% (FOR RCP4.5-HIST AND G3-HIST) AND 95% (G3-RCP4.5), ACCORDING TO THE WILCOXON RANK-SUM TEST.....	44
FIGURE 3-11 IMPACT OF GLOBAL WARMING AND GEOENGINEERING ON HEAT ACCUMULATION (GDH) IN PERIOD1 (A, B, C), AND PERIOD 2 (D, E, F) FOR THE AVERAGE OF HADGEM2-ES AND MPI-ESM-LR OVER HIMACHAL PRADESH, INDIA. THE UNHATCHED AREA SHOWS THAT THE DIFFERENCE OF GDH FOR THE GIVEN SCENARIOS IS STATISTICALLY SIGNIFICANT AT 99% (FOR RCP4.5-HIST AND G3-HIST) AND 95% (G3-RCP4.5), ACCORDING TO THE WILCOXON RANK-SUM TEST.	45
FIGURE 3-12 AGROCLIMATIC SUITABILITY (A, B, AND C) AND LAND SUITABILITY (D, E, AND F) FOR PERIOD1 (2055-2069) OBTAINED FROM THE AVERAGE OF HADGEM2-ES AND MPI-ESM-LR. THE REGIONS HAVING ADEQUATE CLIMATE TO SUPPORT AGRICULTURE IS TERMED AS AGRO-CLIMATICALLY SUITABLE. THE AREA HAVING SUITABLE SOIL (SHOWN AS BLACK DOTS) IS OVERLAID ON A, B AND C. SUITABLE CLIMATE IS COMBINED WITH SUITABLE SOIL TO DELINEATE LAND SUITABILITY. THE SHADED AREA IS THE SUITABLE REGION AND THE WHITE AREA IS THE UNSUITABLE REGION IN (D, E, AND F).....	47

FIGURE 3-13 AGROCLIMATIC SUITABILITY (A, B, AND C) AND LAND SUITABILITY (D, E, AND F) FOR PERIOD2 (2075-2089) OBTAINED FROM THE AVERAGE OF HADGEM2-ES AND MPI-ESM-LR. THE REGIONS HAVING ADEQUATE CLIMATE TO SUPPORT AGRICULTURE IS TERMED AS AGRO-CLIMATICALLY SUITABLE. THE AREA HAVING SUITABLE SOIL (SHOWN AS BLACK DOTS) IS OVERLAID ON A, B AND C. SUITABLE CLIMATE IS COMBINED WITH SUITABLE SOIL TO DELINEATE LAND SUITABILITY. THE SHADED AREA IS THE SUITABLE REGION AND THE WHITE AREA IS UNSUITABLE REGION IN (D, E, AND F).....	49
FIGURE 4-1 AGRO-ECOLOGICAL AND SOCIOECONOMIC CHARACTERISTICS OF UTTAR PRADESH.....	53
FIGURE 4-2 CLIMATE TYPE, PERCENTAGE OF CULTIVATED AND IRRIGATED LAND FOR EACH AEZ OF UTTAR PRADESH (DEPARTMENT OF AGRICULTURE, COOPERATION & FARMERS' WELFARE, GOVERNMENT OF INDIA)	56
FIGURE 4-3 SSP-RCP SCENARIO MATRIX ILLUSTRATING SCENARIO MIP SIMULATIONS. EACH CELL IN THE MATRIX INDICATES A COMBINATION OF SOCIOECONOMIC DEVELOPMENT PATHWAY (I.E., AN SSP) AND CLIMATE OUTCOME BASED ON A PARTICULAR FORCING PATHWAY. FOR EXAMPLE, SCENARIO MATRIX FOR SSP245 IS COMBINATION OF A CLIMATE FORCING (RCP4.5) OF 4.5 W/M2 BY 2100 AND A "MIDDLE OF THE ROAD" (SSP2) SHARED SOCIOECONOMIC PATHWAY (O'NEILL ET AL., 2016).....	58
FIGURE 4-4 TAYLOR DIAGRAMS FOR RAINFALL (A), T_{MAX} (B), T_{MIN} (C) FOR JJAS FROM THE CMIP6 MODELS. THE BLACK DOT ON X-AXIS SHOWS THE OBSERVED DATA; DOTTED-GREEN SEMI-CIRCLES SHOW THE CENTRED ROOT MEAN SQUARE ERROR AND BLACK ARCS SHOW THE NORMALIZED STANDARD DEVIATION.....	63
FIGURE 4-5 DESIGN AND FLOW OF CERES-RICE MODEL INPUTS AND NUMERICAL EXPERIMENTS	65
FIGURE 4-6 COMPARISON OF SEASONAL MEAN A) T_{MAX} , B) T_{MIN} , C) ANTHESIS AND D) MATURITY FROM IMD AND CMIP6 GCM FORCED CERES-RICE MODEL FOR THE PERIOD (1994–2014) AGGREGATED FOR AEZs. ANTHESIS AND MATURITY DUARTION ARE IN THE UNIT OF DAP (DAYS AFTER PLANTING). SEASONAL STANDS FOR A CROP SEASON STARTING FROM PLANTING AND ENDING AT MATURITY. A BOX-PLOT IS SHOWN FOR EVERY AEZ REPRESENTING THE SPATIOTEMPORAL AVERAGE FOR THE BASELINE PERIOD OVER EACH AEZ FOR ALL 16 GCMs, THUS DEPICTING THE INTER-MODEL SPREAD. BLUE AND RED LINES ARE THE AVERAGE VALUE OVER EVERY AEZ FOR IMD AND MMM, RESPECTIVELY. ENCIRCLED BLACK DOT DEPICTS THE MEDIAN OF THE DATA, THE LOWER AND UPPER EDGES OF THE SOLID BOXES ARE 25TH AND 75TH PERCENTILES, RESPECTIVELY, HAVING A LINE ATTACHED TO IT, EXTENDING UP TO THE MINIMUM AND MAXIMUM VALUES EXCLUDING OUTLIERS. RED DOTS ARE THE OUTLIERS.	67
FIGURE 4-7 COMPARISON OF SEASONAL MEAN A) RAINFALL (MM) AND B) IRRIGATION (MM) FROM IMD AND CMIP6 GCM FORCED CERES-RICE MODEL FOR THE PERIOD (1995–2014) AGGREGATED FOR EACH AEZ. SEASONAL STANDS FOR A CROP SEASON STARTING FROM PLANTING AND ENDING AT MATURITY. THE BOX PLOTS ARE SIMILAR TO FIGURE 4-4.	69
FIGURE 4-8 COMPARISON OF SEASONAL MEAN RICE TRANSPIRATION (EP) FOR A) IRRIGATED RICE AND B) RAINFED RICE FROM IMD AND CMIP6 GCM FORCED CERES-RICE MODEL FOR THE PERIOD (1995–2014) AGGREGATED FOR EACH AEZ. SEASONAL STANDS FOR A CROP SEASON STARTING FROM PLANTING AND ENDING AT MATURITY.....	70
FIGURE 4-9 COMPARISON OF SEASONAL MEAN SOIL EVAPORATION (ES) FOR A) IRRIGATED RICE AND B) RAINFED RICE FROM IMD AND CMIP6 GCM FORCED CERES-RICE MODEL FOR THE PERIOD (1995–2014) AGGREGATED FOR EACH AEZ. SEASONAL STANDS FOR A CROP SEASON STARTING FROM PLANTING AND ENDING AT MATURITY.....	71
FIGURE 4-10 COMPARISON OF SEASONAL MEAN EVAPOTRANSPIRATION (ET) FOR A) IRRIGATED RICE AND B) RAINFED RICE FROM IMD AND CMIP6 GCM FORCED CERES-RICE MODEL FOR THE PERIOD (1995–2014) AGGREGATED FOR EACH AEZ. SEASONAL STANDS FOR A CROP SEASON STARTING FROM PLANTING AND ENDING AT MATURITY.....	72

FIGURE 4-11 COMPARISON OF SEASONAL MEAN YIELD FOR A) IRRIGATED RICE AND B) RAINFED RICE FROM IMD AND CMIP6 GCM FORCED CERES-RICE MODEL FOR THE PERIOD (1995–2014) AGGREGATED FOR EACH AEZ. SEASONAL STANDS FOR A CROP SEASON STARTING FROM PLANTING AND ENDING AT MATURITY.	73
FIGURE 4-12 COMPARISON OF SEASONAL MEAN WUE FOR A) IRRIGATED RICE AND B) RAINFED RICE FROM IMD AND CMIP6 GCM FORCED CERES-RICE MODEL FOR THE PERIOD (1995–2014) AGGREGATED FOR EACH AEZ. SEASONAL STANDS FOR A CROP SEASON STARTING FROM PLANTING AND ENDING AT MATURITY.	74
FIGURE 5-1 CHANGES IN SEASONAL T_{MAX} FOR (I) SSP245 AND (II) SSP585 IS PLOTTED. SUBFIGURES I AND II SHOW HISTORICAL (A, E, I), AND CHANGES FOR 2026-2035 (B, F, J), 2046-2055 (C, G, K), AND 2090-2099 (D, H, L) FOR EARLY-PLANTING (FIRST AND FOURTH ROW), MID-PLANTING (SECOND AND FIFTH ROW), AND LATE PLANTING (THIRD AND SIXTH ROW). OVERLAID BLACK DOTS REPRESENT MODEL AGREEMENT (75% OF MODELS) ON SIGN OF CHANGE. BLACK CONTOURS SHOW INTER-MODEL STANDARD DEVIATION OF 16 CMIP6 GCMs.	81
FIGURE 5-2 CHANGES IN SEASONAL T_{MIN} FOR (I) SSP245 AND (II) SSP585 ARE SHOWN. SUBFIGURES I AND II SHOW HISTORICAL (A, E, I), AND CHANGES FOR 2026-2035 (B, F, J), 2046-2055 (C, G, K), AND 2090-2099 (D, H, L) FOR EARLY-PLANTING (FIRST AND FOURTH ROW), MID-PLANTING (SECOND AND FIFTH ROW), AND LATE PLANTING (THIRD AND SIXTH ROW). OVERLAID BLACK DOTS REPRESENT MODEL AGREEMENT (75% OF MODELS) ON SIGN OF CHANGE. BLACK CONTOURS SHOW INTER-MODEL STANDARD DEVIATION OF 16 CMIP6 GCMs.	83
FIGURE 5-3 CHANGES IN SEASONAL ANTHESIS DURATION FOR (I) SSP245 AND (II) SSP585 ARE SHOWN. SUBFIGURES I AND II SHOW HISTORICAL (A, E, I), AND CHANGES FOR 2026-2035 (B, F, J), 2046-2055 (C, G, K), AND 2090-2099 (D, H, L) FOR EARLY-PLANTING (FIRST AND FOURTH ROW), MID-PLANTING (SECOND AND FIFTH ROW), AND LATE PLANTING (THIRD & SIXTH ROW). OVERLAID BLACK DOTS REPRESENT MODEL AGREEMENT (75% OF MODELS) ON SIGN OF CHANGE. BLACK CONTOURS SHOW INTER-MODEL STANDARD DEVIATION OF 16 CMIP6 GCMs.	84
FIGURE 5-4 CHANGES IN SEASONAL MATURITY DURATION FOR (I) SSP245 AND (II) SSP585 ARE SHOWN. SUBFIGURES I AND II SHOW HISTORICAL (A, E, I), AND CHANGES FOR 2026-2035 (B, F, J), 2046-2055 (C, G, K), AND 2090-2099 (D, H, L) FOR EARLY-PLANTING (FIRST AND FOURTH ROW), MID-PLANTING (SECOND AND FIFTH ROW), AND LATE PLANTING (THIRD AND SIXTH ROW). OVERLAID BLACK DOTS REPRESENT MODEL AGREEMENT (75% OF MODELS) ON SIGN OF CHANGE. BLACK CONTOURS SHOW INTER-MODEL STANDARD DEVIATION OF 16 CMIP6 GCMs.	85
FIGURE 5-5 CHANGES IN SEASONAL RAINFALL FOR (I) SSP245 AND (II) SSP585 ARE SHOWN. SUBFIGURES I AND II SHOW HISTORICAL (A, E, I), AND CHANGES FOR 2026-2035 (B, F, J), 2046-2055 (C, G, K), AND 2090-2099 (D, H, L) FOR EARLY-PLANTING (FIRST AND FOURTH ROW), MID-PLANTING (SECOND AND FIFTH ROW), AND LATE PLANTING (THIRD AND SIXTH ROW). OVERLAID BLACK DOTS REPRESENT MODEL AGREEMENT (75% OF MODELS) ON SIGN OF CHANGE. BLACK CONTOURS SHOW INTER-MODEL STANDARD DEVIATION OF 16 CMIP6 GCMs.	87
FIGURE 5-6 CHANGES IN SEASONAL IRRIGATED RICE ET FOR (I) SSP245 AND (II) SSP585 ARE SHOWN. SUBFIGURES I AND II SHOW HISTORICAL (A, E, I), AND CHANGES FOR 2026-2035 (B, F, J), 2046-2055 (C, G, K), AND 2090-2099 (D, H, L) FOR EARLY-PLANTING (FIRST AND FOURTH ROW), MID-PLANTING (SECOND AND FIFTH ROW), AND LATE PLANTING (THIRD AND SIXTH ROW). OVERLAID BLACK DOTS REPRESENT MODEL AGREEMENT (75% OF MODELS) ON SIGN OF CHANGE. BLACK CONTOURS SHOW INTER-MODEL STANDARD DEVIATION OF 16 CMIP6 GCMs.	88
FIGURE 5-7 CHANGES IN SEASONAL IRRIGATION AMOUNT FOR (I) SSP245 AND (II) SSP585 ARE PLOTTED. SUBFIGURES I AND II SHOW HISTORICAL (A, E, I), AND CHANGES FOR 2026-2035 (B, F, J), 2046-2055 (C, G, K), AND 2090-2099 (D, H, L) FOR EARLY-	

PLANTING (FIRST AND FOURTH ROW), MID-PLANTING (SECOND AND FIFTH ROW), AND LATE PLANTING (THIRD AND SIXTH ROW). OVERLAID BLACK DOTS REPRESENT MODEL AGREEMENT (75% OF MODELS) ON SIGN OF CHANGE. BLACK CONTOURS SHOW INTER-MODEL STANDARD DEVIATION OF 16 CMIP6 GCMs. 90

FIGURE 5-8 CHANGES IN SEASONAL RAINFED RICE ET FOR (I) SSP245 AND (II) SSP585 ARE PLOTTED. SUBFIGURES I AND II SHOW HISTORICAL (A, E, I), AND CHANGES FOR 2026-2035 (B, F, J), 2046-2055 (C, G, K), AND 2090-2099 (D, H, L) FOR EARLY-PLANTING (FIRST AND FOURTH ROW), MID-PLANTING (SECOND AND FIFTH ROW), AND LATE PLANTING (THIRD AND SIXTH ROW). OVERLAID BLACK DOTS REPRESENT MODEL AGREEMENT (75% OF MODELS) ON SIGN OF CHANGE. BLACK CONTOURS SHOW INTER-MODEL STANDARD DEVIATION OF 16 CMIP6 GCMs. 92

FIGURE 5-9 CHANGES IN IRRIGATED RICE YIELD FOR (I) SSP245 AND (II) SSP585 ARE SHOWN. SUBFIGURES I AND II SHOW HISTORICAL (A, E, I), AND CHANGES FOR 2026-2035 (B, F, J), 2046-2055 (C, G, K), AND 2090-2099 (D, H, L) FOR EARLY-PLANTING (FIRST AND FOURTH ROW), MID-PLANTING (SECOND AND FIFTH ROW), AND LATE PLANTING (THIRD AND SIXTH ROW). OVERLAID BLACK DOTS REPRESENT MODEL AGREEMENT (75% OF MODELS) ON SIGN OF CHANGE. BLACK CONTOURS SHOW INTER-MODEL STANDARD DEVIATION OF 16 CMIP6 GCMs. 94

FIGURE 5-10 CHANGES IN IRRIGATED RICE YIELD (AVERAGED IN SPACE FOR EACH AEZ AND IN TIME FOR EACH 10-YEAR PERIOD) IN A) EARLY-SEASON PLANTING, B) MID-SEASON PLANTING, AND C) LATE-SEASON FOR 2026-2035, 2046-2055 AND 2090-2099 UNDER SSP245 AND SSP585 AGGREGATED FOR EACH AEZ (AS CAN BE SEEN FROM LEGEND). THE BOX PLOT FOR EACH AEZ SHOWS CHANGES IN PROJECTED YIELDS FROM 16 CMIP6 GCMs. THE FIRST THREE PANELS (SEPARATED BY BLACK DASHED VERTICAL LINE) OF EACH SUBPLOT REPRESENTS THE THREE FUTURE PERIODS OF SSP245 AND NEXT THREE PANELS REPRESENT THE SAME FOR SSP585. 95

FIGURE 5-11 CHANGES IN RAINFED RICE YIELD FOR (I) SSP245 AND (II) SSP585 ARE SHOWN. SUBFIGURES I AND II SHOW HISTORICAL (A, E, I), AND CHANGES FOR 2026-2035 (B, F, J), 2046-2055 (C, G, K), AND 2090-2099 (D, H, L) FOR EARLY-PLANTING (FIRST AND FOURTH ROW), MID-PLANTING (SECOND AND FIFTH ROW), AND LATE PLANTING (THIRD AND SIXTH ROW). OVERLAID BLACK DOTS REPRESENT MODEL AGREEMENT (75% OF MODELS) ON SIGN OF CHANGE. BLACK CONTOURS SHOW INTER-MODEL STANDARD DEVIATION OF 16 CMIP6 GCMs. 96

FIGURE 5-12 CHANGES IN RAINFED RICE YIELD (AVERAGED IN SPACE FOR EACH AEZ AND IN TIME FOR EACH 10-YEAR PERIOD) IN A) EARLY-SEASON PLANTING, B) MID-SEASON PLANTING, AND C) LATE-SEASON FOR 2026-2035, 2046-2055 AND 2090-2099 UNDER SSP245 AND SSP585 AGGREGATED FOR EACH AEZ (AS CAN BE SEEN FROM LEGEND). THE BOX PLOT FOR EACH AEZ SHOWS CHANGES IN PROJECTED YIELDS FROM 16 CMIP6 GCMs. THE FIRST THREE PANELS (SEPARATED BY BLACK DASHED VERTICAL LINE) OF EACH SUBPLOT REPRESENTS THE THREE FUTURE PERIODS OF SSP245 AND NEXT THREE PANELS REPRESENT THE SAME FOR SSP585. 97

FIGURE 5-13 CHANGES IN IRRIGATED RICE WUE FOR (I) SSP245 AND (II) SSP585 ARE SHOWN. SUBFIGURES I AND II SHOW HISTORICAL (A, E, I), AND CHANGES FOR 2026-2035 (B, F, J), 2046-2055 (C, G, K), AND 2090-2099 (D, H, L) FOR EARLY-PLANTING (FIRST AND FOURTH ROW), MID-PLANTING (SECOND AND FIFTH ROW), AND LATE PLANTING (THIRD AND SIXTH ROW). OVERLAID BLACK DOTS REPRESENT MODEL AGREEMENT (75% OF MODELS) ON SIGN OF CHANGE. BLACK CONTOURS SHOW INTER-MODEL STANDARD DEVIATION OF 16 CMIP6 GCMs. 98

FIGURE 5-14 CHANGES IN RAINFED RICE WUE FOR (I) SSP245 AND (II) SSP585 ARE SHOWN. SUBFIGURES I AND II SHOW HISTORICAL (A, E, I), AND CHANGES FOR 2026-2035 (B, F, J), 2046-2055 (C, G, K), AND 2090-2099 (D, H, L) FOR EARLY-PLANTING (FIRST AND FOURTH ROW), MID-PLANTING (SECOND AND FIFTH ROW), AND LATE PLANTING (THIRD AND SIXTH ROW). OVERLAID BLACK

DOTS REPRESENT MODEL AGREEMENT (75% OF MODELS) ON SIGN OF CHANGE. BLACK CONTOURS SHOW INTER-MODEL STANDARD DEVIATION OF 16 CMIP6 GCMs.	100
FIGURE 5-15 COMPARING CO ₂ FERTILIZATION EFFECT ON PERCENTAGE CHANGE IN YIELD FROM HISTORICAL IN IRRIGATED (I) AND RAINFED RICE (II) FOR MID-SEASON PLANTING. SUBFIGURES I AND II SHOW RICE YIELD FOR TRANSIENT CO ₂ CONCENTRATION AND CLIMATE OF SSP245 (A, E, I), 2005 CO ₂ CONCENTRATION AND CLIMATE OF SSP245 (B, F, J), TRANSIENT CO ₂ CONCENTRATION AND CLIMATE OF SSP585 (C, G, K), AND 2005 CO ₂ CONCENTRATION AND CLIMATE OF SSP585 (D, H, L) FOR 2026-2035 (FIRST AND FOURTH ROW), 2046-2055 (SECOND AND FIFTH ROW), AND 2090-2099 (THIRD AND SIXTH ROW). OVERLAID BLACK DOTS REPRESENT MODEL AGREEMENT (75% OF MODELS) ON SIGN OF CHANGE. BLACK CONTOURS SHOW INTER-MODEL STANDARD DEVIATION OF 16 CMIP6 GCMs.	102
FIGURE 5-16 AVERAGE PERCENTAGE CHANGES IN TMAX, TMIN, RAINFALL, CO ₂ , LGP, ET, IRRIGATION (IR), YIELD (YD), AND WUE FOR 2030s, 2050s AND 2090s UNDER SSP245 AND SSP585 OVER UTTAR PRADESH. ADJACENT TO MEAN PERCENTAGE CHANGE ARE RANGE OF GCM UNCERTAINTIES IN CERES-RICE OUTPUTS.	103
FIGURE A1 DAILY MAXIMUM TEMPERATURE (A, B, C), DAILY MEAN TEMPERATURE (D, E, F), AND DAILY MINIMUM TEMPERATURE (G, H, I) FOR PRINCETON GLOBAL FORCING DATA, HADGEM2-ES AND MPI-ESM-LR RESPECTIVELY.....	130
FIGURE A2 IMPACT OF GLOBAL WARMING AND GEOENGINEERING ON CHILL ACCUMULATION (CP) IN THE PERIOD1 (2055-2069) FOR HADGEM2-ES (A, B, C) AND MPI-ESM-LR (D, E, F) OVER HIMACHAL PRADESH, INDIA. THE UNHATCHED AREA SHOWS THAT THE DIFFERENCE OF CP FOR THE GIVEN SCENARIOS IS STATISTICALLY SIGNIFICANT AT 99% (FOR RCP4.5-HIST AND G3-HIST) AND 95% (G3-RCP4.5), ACCORDING TO THE WILCOXON RANK-SUM TEST.	131
FIGURE A3 IMPACT OF GLOBAL WARMING AND GEOENGINEERING ON CHILL ACCUMULATION (CP) IN THE PERIOD2 (2075-2089) FOR HADGEM2-ES (A, B, C) AND MPI-ESM-LR (D, E, F) OVER HIMACHAL PRADESH, INDIA. THE UNHATCHED AREA SHOWS THAT THE DIFFERENCE OF CP FOR THE GIVEN SCENARIOS IS STATISTICALLY SIGNIFICANT AT 99% (FOR RCP4.5-HIST AND G3-HIST) AND 95% (G3-RCP4.5), ACCORDING TO THE WILCOXON RANK-SUM TEST.	132
FIGURE A4 IMPACT OF GLOBAL WARMING AND GEOENGINEERING ON HEAT ACCUMULATION (GDH) IN THE PERIOD1 (2055-2069) FOR HADGEM2-ES (A, B, C) AND MPI-ESM-LR (D, E, F) OVER HIMACHAL PRADESH, INDIA. THE UNHATCHED AREA SHOWS THAT THE DIFFERENCE OF CP FOR THE GIVEN SCENARIOS IS STATISTICALLY SIGNIFICANT AT 99% (FOR RCP4.5-HIST AND G3-HIST) AND 95% (G3-RCP4.5), ACCORDING TO THE WILCOXON RANK-SUM TEST.	133
FIGURE A5 IMPACT OF GLOBAL WARMING AND GEOENGINEERING ON HEAT ACCUMULATION (GDH) IN THE PERIOD2 (2075-2089) FOR HADGEM2-ES (A, B, C) AND MPI-ESM-LR (D, E, F) OVER HIMACHAL PRADESH, INDIA. THE UNHATCHED AREA SHOWS THAT THE DIFFERENCE OF CP FOR THE GIVEN SCENARIOS IS STATISTICALLY SIGNIFICANT AT 99% (FOR RCP4.5-HIST AND G3-HIST) AND 95% (G3-RCP4.5), ACCORDING TO THE WILCOXON RANK-SUM TEST	134
FIGURE A6 AGROCLIMATIC SUITABILITY (A, B, AND C) AND LAND SUITABILITY (D, E, AND F) FOR THE PERIOD1 (2055-2069) OBTAINED FROM THE MODEL HADGEM2-ES. THE REGIONS HAVING ADEQUATE CLIMATE TO SUPPORT AGRICULTURE IS TERMED AS AGROCLIMATICALLY SUITABLE. THE AREA HAVING SUITABLE SOIL (SHOWN AS BLACK DOTS AT 25 KM RESOLUTION) IS OVERLAID ON A, B AND C. SUITABLE CLIMATE IS COMBINED WITH SUITABLE SOIL TO DELINEATE LAND SUITABILITY. THE SHADED AREA IS THE SUITABLE REGION, AND THE WHITE AREA IS THE UNSUITABLE REGION.....	135
FIGURE A7 AGROCLIMATIC SUITABILITY (A, B, AND C) AND LAND SUITABILITY (D, E, AND F) FOR THE PERIOD1 (2055-2069) OBTAINED FROM THE MODEL MPI-ESM-LR. THE REGIONS HAVING ADEQUATE CLIMATE TO SUPPORT AGRICULTURE IS TERMED AS AGROCLIMATICALLY SUITABLE. THE AREA HAVING SUITABLE SOIL (SHOWN AS BLACK DOTS AT 25 KM RESOLUTION) IS OVERLAID ON A, B	

AND C. SUITABLE CLIMATE IS COMBINED WITH SUITABLE SOIL TO DELINEATE LAND SUITABILITY. THE SHADED AREA IS THE SUITABLE REGION, AND THE WHITE AREA IS THE UNSUITABLE REGION.....	136
FIGURE A8 AGROCLIMATIC SUITABILITY (A, B, AND C) AND LAND SUITABILITY (D, E, AND F) FOR THE PERIOD2 (2075-2089) OBTAINED FROM THE MODEL HADGEM2-ES. THE REGIONS HAVING ADEQUATE CLIMATE TO SUPPORT AGRICULTURE IS TERMED AS AGROCLIMATICALLY SUITABLE. THE AREA HAVING SUITABLE SOIL (SHOWN AS BLACK DOTS AT 25 KM RESOLUTION) IS OVERLAID ON A, B AND C. SUITABLE CLIMATE IS COMBINED WITH SUITABLE SOIL TO DELINEATE LAND SUITABILITY. THE SHADED AREA IS THE SUITABLE REGION, AND THE WHITE AREA IS THE UNSUITABLE REGION.....	137
FIGURE A9 AGROCLIMATIC SUITABILITY (A, B, AND C) AND LAND SUITABILITY (D, E, AND F) FOR THE PERIOD2 (2075-2089) OBTAINED FROM THE MODEL MPI-ESM-LR. THE REGIONS HAVING ADEQUATE CLIMATE TO SUPPORT AGRICULTURE IS TERMED AS AGROCLIMATICALLY SUITABLE. THE AREA HAVING SUITABLE SOIL (SHOWN AS BLACK DOTS AT 25 KM RESOLUTION) IS OVERLAID ON A, B AND C. SUITABLE CLIMATE IS COMBINED WITH SUITABLE SOIL TO DELINEATE LAND SUITABILITY. THE SHADED AREA IS THE SUITABLE REGION, AND THE WHITE AREA IS THE UNSUITABLE REGION.....	138
FIGURE A10 CHANGES IN SEASONAL IRRIGATED RICE EP FOR (I) SSP245 AND (II) SSP585 ARE SHOWN. SUBFIGURES I AND II SHOW HISTORICAL (A, E, I), AND CHANGES FOR 2026-2035 (B, F, J), 2046-2055 (C, G, K), AND 2090-2099 (D, H, L) FOR EARLY-PLANTING (FIRST AND FOURTH ROW), MID-PLANTING (SECOND AND FIFTH ROW), AND LATE PLANTING (THIRD AND SIXTH ROW). OVERLAID BLACK DOTS REPRESENT MODEL AGREEMENT (75% OF MODELS) ON SIGN OF CHANGE. BLACK CONTOURS SHOW INTER-MODEL STANDARD DEVIATION OF 16 CMIP6 GCMS.....	139
FIGURE A11 CHANGES IN SEASONAL IRRIGATED RICE ES FOR (I) SSP245 AND (II) SSP585 ARE SHOWN. SUBFIGURES I AND II SHOW HISTORICAL (A, E, I), AND CHANGES FOR 2026-2035 (B, F, J), 2046-2055 (C, G, K), AND 2090-2099 (D, H, L) FOR EARLY-PLANTING (FIRST AND FOURTH ROW), MID-PLANTING (SECOND AND FIFTH ROW), AND LATE PLANTING (THIRD AND SIXTH ROW). OVERLAID BLACK DOTS REPRESENT MODEL AGREEMENT (75% OF MODELS) ON SIGN OF CHANGE. BLACK CONTOURS SHOW INTER-MODEL STANDARD DEVIATION OF 16 CMIP6 GCMS.....	140
FIGURE A12 RELATION BETWEEN RAINED RICE ET CHANGE AND YIELD CHANGE.....	141

List of Tables

TABLE 2-1 MAXIMUM, MINIMUM, MEAN VALUES OF 99 TH PERCENTILE OF THE VALIDATION PERIOD (2000-2009) FOR OBSERVATION, QM, KNN _p , KNN, AND SVM-KNN	24
TABLE 3-1 SPATIAL RANGE OF DIFFERENCES IN MAXIMUM, MEAN, AND MINIMUM TEMPERATURES BETWEEN RCP4.5 AND G3 SIMULATIONS AVERAGED FOR THE END OF THE GEOENGINEERING PERIOD (1) AND THE END OF THE TERMINATION PERIOD (2) FOR HIMACHAL PRADESH, INDIA.	41
TABLE 3-2 SPATIAL RANGE OF DIFFERENCES IN WINTER CHILL (CP) AND GROWING DEGREE HOURS (GDH) BETWEEN HISTORICAL, RCP4.5, AND G3 SIMULATIONS AVERAGED FOR THE END OF THE GEOENGINEERING PERIOD (1) AND THE END OF THE TERMINATION PERIOD (2) FOR HIMACHAL PRADESH, INDIA.	46
TABLE 4-1 GCMs INFORMATION FROM CMIP6 USED IN THIS STUDY. MODEL HAVING INFORMATION IN SAME COLOURED TEXT (EXCEPT BLACK) BELONGS TO SAME MODELLING GROUP. FOR EXAMPLE, ACCESS-CM2 AND ACCESS-ESM 1-5 ARE BOTH FROM CSIRO, AUSTRALIA.	59
TABLE 4-2 GENETIC COEFFICIENTS OF RICE FROM CALIBRATED AND VALIDATED CERS-RICE MODEL BY AGROMET DIVISION OF IMD FOR UTTAR PRADESH	60
TABLE 4-3 DEFINITION OF RICE GENETIC COEFFICIENTS USED IN CERES-RICE (BUDDHABOON ET AL., 2018)	61
TABLE 4-4 NRMSE, PCC, AND RATIO OF PCC BY NRMSE FOR JJAS DAILY RAINFALL, T _{MAX} , AND T _{MIN} OVER UTTAR PRADESH. THE ROWS ARE SORTED BASED ON PCC/NRMSE RATIO FOR RAINFALL.	62
TABLE 5-1 STUDIES ASSESSING THE IMPACT OF CLIMATE CHANGE ON RICE CROP USING GCM DATA IN CROP MODELS OVER VARIOUS PARTS OF INDIA	78

List of Acronyms

AEZ	Agro-Ecological Zone
AgMIP	Agricultural Model Intercomparison and Improvement Project
BKZ	Bundelkhand Zone
BTZ	Bhabhar and Tarai Zone
CMIP	Climate Model Intercomparison Project
CP	Chill Portions
CPZ	Central Plain Zone
DEM	Digital Elevation Model
DES	Directorate of Economics & Statistics
DSL	Dry Spell Length
DSSAT	Decision Support System for Agrotechnology Transfer
EPZ	Eastern Plain Zone
ET	Evapotranspiration
FACE	free-Air CO ₂ Enrichment
FAOSTAT	Food and Agriculture Organization Corporate Statistical Database
GCM	Global climate models
GDD	Growing Degree Days
GDH	Growing Degree Hours
GeoMIP	Geoengineering Model Intercomparison Project
GGCMI	Global Gridded Crop Model Intercomparison
GHG	Green House Gas
IGP	Indo-Gangetic Plains
IMD	India Meteorological Department
IPCC	Intergovernmental Panel on Climate Change
ISM	Indian summer monsoon
JJAS	June-July-August-September
KNN	K-nearest neighbours
LGP	Length of Growing Period
MLR	Multiple Linear Regression
MMM	Multi-Model Mean
MWZ	Mid-western plain Zone
NBSSLUP	National Bureau for Soil Survey and Land Use Planning
NCEP	National Centre for Environmental Prediction
NEZ	North-Eastern Plain Zone
PCA	Principle Component Analysis

QM	Quantile Mapping
RCM	Regional Climate Model
RCP	Representative Concentration Pathway
SRM	Solar Radiation Management
SRTM	Shuttle Radar Topographic Mission
SSP	Shared Socioeconomic Pathway
SVM	Support Vector Machine
SWZ	Southwestern semi-arid plain Zone
TM	Temperature Model
UNFCCC	United Nations Framework Convention on Climate Change
VZ	Vindhyan Zone
WDF	Wet Day Fraction
WG	Working Group
WPZ	Western Plain Zone
WSL	Wet Spell Length
WUE	Water Use Efficiency